

Nonlinear Pulse Propagation in Dispersion-Decreasing Fiber Studied with Frequency-Resolved Optical Gating

N. K. Fontaine, R. P. Scott, W. Cong,
B. H. Kolner, J. P. Heritage and S. J. Ben Yoo

*Department of Applied Science, Department of Electrical and Computer Engineering,
University of California, Davis, One Shields Avenue, Davis, California 95616
nkfontaine@ucdavis.edu*

Abstract: We investigate pulse propagation in a dispersion-decreasing fiber over a wide range of input powers both theoretically, and experimentally using frequency-resolved optical gating. Our simulations and experiments verify significant influence of Raman scattering on pulse propagation.

©2005 Optical Society of America

OCIS codes: (320.7100) Ultrafast measurements; (060.5530) Pulse propagation and solitons; (320.5520) Pulse compression

1. Introduction

Previous research in optical pulse compression at 1550 nm using dispersion-decreasing fibers (DDF) has been primarily concerned with time-domain pulse quality, specifically minimization of the pedestal surrounding the pulse [1]. In our spectral phase-encoded version of an optical code division multiple access (O-CDMA) communications testbed [2], we have found that it is not only necessary to have a short, well-behaved pulse in the time domain, but the spectrum must also be clean (i.e., significant deviation from a Fourier transform-limited spectrum markedly degrades the bit-error-rate (BER) performance). In recent work by Fatemi [3], characterization of compressed pulses with frequency resolved optical gating (FROG) from a short 100-m fiber over a narrow range of pulse energies (11–18 pJ) was considered. In contrast, we present here studies of nonlinear pulse propagation in much longer (1 km) DDF over a wide range of input pulse energies from 4 pJ to 27 pJ corresponding to soliton numbers $N=1.4$ to $N=3.7$. Qualitatively, we find that for low input energies, (<10 pJ), the pulse compresses very fast as the input energy increases. In the range from 10 pJ to 25 pJ the pulse is compressed to approximately 0.3 ps. Above ≈ 25 pJ the compressed pulse splits into two and these begin propagating at different group velocities. Also, we observe the spectrum shift due to the higher order nonlinear effects (primarily from the noninstantaneous Raman vibrational nonlinear response) to emerge at higher powers. At these higher pulse energies propagating in longer fibers, the complex temporal and spectral reshaping must be accurately modeled in order to prepare high-quality pulses for O-CDMA communications systems.

2. Experimental Description

Our experiments use a 1550-nm modelocked fiber laser (PriTel UOC-3) to generate 2.5-ps pulses at a 9.95-GHz rate. These pulses are amplified by an erbium-doped fiber amplifier (EDFA) (PriTel FA-22) to output energies between 3 pJ and 30 pJ. These are then launched into a 1-km dispersion-decreasing fiber (DDF) (PriTel DD-400) and the output complex electric field is studied as a function of pulse energy with second harmonic generation (SHG) FROG. Our FROG system uses a non-collinear SHG autocorrelator with a 2-mm LiNbO₃ crystal phase matched at 1550 nm. The spectrometer and detector (2D-CCD array) used to analyze the SHG light have a spectral bandwidth of 17 nm, resolution bandwidth of 0.05 nm, and a dynamic range of ≈ 16 bits. The spectral calibration was realized by comparing the FROG frequency marginal with the autoconvolution of the pulse spectrum [4].

The FROG traces were prepared by subtracting the mean of the background, low pass filtering, corner suppressing as described in [5], and were spline-interpolated onto either a 128×128 or 256×256 grid depending on their complexity. The algorithm typically achieved a FROG retrieval error of $G = 0.0025$ for the less complex traces indicating good convergence of FROG algorithm. More complicated traces converged to $G = 0.007$, but the retrieved fields still matched well with theory so we include them in our analysis. We believe the slight increase in G is due to some clipping of the weak temporal wings at the edges of the scan window. The direction of time ambiguity was removed by simulating the pulse propagation through the DDF and comparing the simulated and measured output spectra. Only one temporal orientation resulted in agreement.

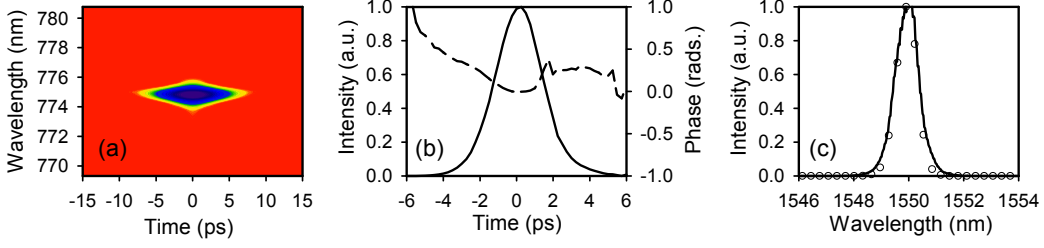


Fig. 1. (a) Measured FROG trace of amplified PriTel oscillator output (input to DDF). (b) Retrieved electric field intensity (solid) and phase (dashed). (c) Measured spectrum (solid curve) and retrieved spectral intensity (circles).

To compare experiment to theory, we used the one-dimensional nonlinear Schrödinger equation (NLSE) including the Raman response function and third-order dispersion (TOD). The nonlinearity is accounted for by defining a response function $R(T) = (1 - f_R)\delta(t) + f_R h_R(t)$ which includes both the instantaneous (electronic) and noninstantaneous (Raman-active vibrational) contributions [6, 7], where f_R defines the fraction of the noninstantaneous to the instantaneous response [8]. The NLSE was integrated using the split-step Fourier method.

Detailed information regarding the dispersion and nonlinear parameters of the DDF was incomplete due, in part, to the variability of the manufacturing process. However, we were provided with approximate values of input and output dispersion ($D \approx 12$ ps/nm/km and ≈ 0 ps/nm/km, respectively), a typical loss of 1.5 dB, and the fact that the fiber has a linear taper. Using these values, and the measured input pulse as a starting point, we chose the other unknown parameters such that our simulations matched experimental data over the entire range of input powers. Thus, we modeled the DDF as having linearly-decreasing group velocity between $\beta_2 = -11.7$ ps²/km and $\beta_2 = -2.5$ ps²/km, a constant TOD parameter of $\beta_3 = 0.116$ ps³/km, a nonlinear parameter of $\gamma = 2.2$ (W·km)⁻¹, and an attenuation of $\alpha = 0.9$ dB/km. As we will show, the simulations gave good qualitative agreement over the entire input power range.

3. Results and Discussion

Fig. 1 presents measured data which fully characterizes the amplified oscillator pulse (used as input to DDF). Fig. 1(a) is the retrieved FROG trace and Fig. 1(b) shows the retrieved electric field intensity profile with phase. The pulse width is 2.9-ps (FWHM) and we can see a small amount of residual phase. The time-bandwidth product is 0.348, near the transform limit of a hyperbolic-secant pulse. The retrieved spectrum in Fig. 1(c) shows a close match to that measured using a commercial optical spectrum analyzer.

Fig. 2(a) shows the evolution of the retrieved temporal envelope of the DDF output pulses with input pulse energies between 4 pJ and 27 pJ. Note the wide range of input pulse energies over which the temporal

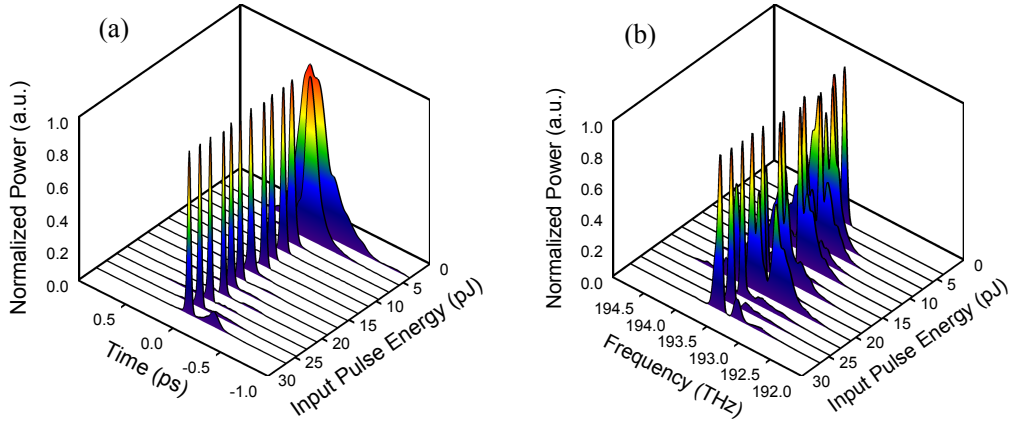


Fig. 2. Data retrieved from SHG FROG measurements of the DDF output. The temporal intensity (a) and spectral intensity (b) as a function of input pulse energy. The direction of pulse energy variation was chosen for plot clarity.

envelope remains approximately unchanged but the spectrum changes rapidly (Fig. 2(b)). Although there seems to be relatively good compression across a large range of powers, only a limited set of these pulses perform well in our O-CDMA testbed. Fig. 3(a) shows one such pulse, while Fig. 3(b) shows a pulse that does not perform well, typically causing the BER to degrade by several orders of magnitude. We are currently trying to isolate the exact cause of the BER increase.

Although we could not find an exact fit to the parameters of the DDF, our success in modeling the DDF through simulations is shown in Fig. 3. Significant spectral and temporal shifts can be seen at higher output powers which show the effects of the Raman component of the nonlinear response. Although not shown, the corresponding measured electric field at 27 pJ matches well with the simulation that includes the stimulated Raman.

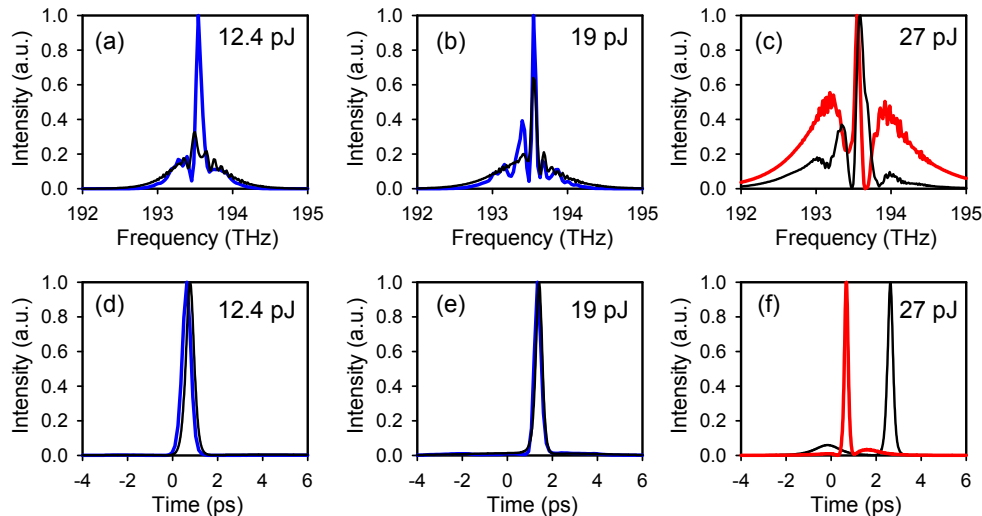


Fig. 3. DDF output for three input pulse energies. (a)–(c) are spectral intensities and (d)–(f) are electric field intensities with simulated data in black and retrieved data in blue. (c) and (f) show simulations with (black) and without (red) stimulated Raman included.

4. Conclusion

Beginning only with values for the input and output linear dispersions, the input pulse shape, and many different measured output pulses corresponding to different input pulse energies, we deduced the nonlinear dispersions and verified the necessity of including Raman interactions to model the DDF. Close agreement between the SHG FROG measured DDF output pulses and simulations will allow us to now use these fiber parameters to model any input pulse and search for better operating regimes for our O-CDMA testbed.

References

1. M. D. Pelusi and L. Hai-Feng, “Higher order soliton pulse compression in dispersion-decreasing optical fibers,” *IEEE J. Quantum Electron.* **33**(8), 1430–1439 (1997).
2. V. J. Hernandez et al., “Spectral phase encoded time spreading (SPECTS) optical code division multiple access for terabit optical access networks,” *J. Lightwave Technol.* **22**(11), 2671–2679 (2004).
3. F. K. Fatemi, “Analysis of nonadiabatically compressed pulses from dispersion-decreasing fiber,” *Opt. Lett.* **27**(18), 1637–1639 (2002).
4. R. Trebino, *Frequency-resolved optical gating: the measurement of ultrashort laser pulses* (Kluwer Academic Publishers, Boston, 2000).
5. D. N. Fittinghoff, K. W. DeLong, R. Trebino and C. L. Ladera, “Noise sensitivity in frequency-resolved optical gating,” *J. Opt. Soc. Amer. B* **12**(10), 1955–1967 (1995).
6. R. Stolen and J. Gordon, “Raman response function of silica-core fibers,” *J. Opt. Soc. Amer. B* **6**(6), 1159–1166 (1989).
7. D. Hollenbeck and C. D. Cantrell, “Multiple-vibrational-mode model for fiber-optic raman gain,” *J. Opt. Soc. Amer. B* **19**(12), 2887–2892 (2002).
8. G. P. Agrawal, *Nonlinear Fiber Optics* (Academic Press, San Diego, 2001).

This work was supported in part by DARPA and SPAWAR under agreement N66001-02-1-8937 and by the AFOSR through the UC Davis Center for Digital Security. The authors would like to thank PriTel, Inc. for their assistance with this work.